A NOVEL EPSILON NEAR ZERO (ENZ) TUNNELING CIRCUIT USING MICROSTRIP TECHNOLOGY FOR HIGH INTEGRABILITY APPLICATIONS

D. V. B. Murthy, A. Corona-Chávez and J. L. Olvera-Cervantes

Large Millimeter Telescope
National Institute of Astrophysics, Optics and Electronics
(I.N.A.O.E)
Puebla-72840, Mexico

Abstract—A novel compact Epsilon Near Zero (ENZ) tunneling circuit with microstrip coupling for high integrability applications is presented. Full design procedure, simulation and experimental results are shown, and a methodology to extract the effective permittivity and propagation constants in the tunnel is described. Detailed analysis of the dependence on external quality factor and tunnel to feed height ratio is investigated. Simulation and measurement results of the ENZ tunnel structure are in good agreement.

1. INTRODUCTION

Metamaterials are artificial composite materials with negative values of permittivity and permeability/either permittivity or permeability are negative which exhibit extraordinary electromagnetic (EM) properties and have attracted much attention in physics and engineering in the past few years. Recently ε-near-zero (ENZ) metamaterials have received much attention for several interesting phenomena like supercoupling, transparency and cloaking devices and pattern reshaping at microwave and optical frequencies [1–3]. The rapid growth and excitement of ENZ materials was due to their ability to achieve very long wavelength in zero permittivity material, allowing propagation in a static-like manner. Engheta et al. [4], explained theoretically the effect of supercoupling, squeezing wave energy, and

field confinement in narrow channels and tight bends using ε-near-zero metamaterials. Brain Edwards et al. [5], proved Epsilon-Near-Zero metamaterial coupling and energy squeezing effect experimentally using a microwave waveguide. To date, ENZ tunnels have been realized with waveguide feeds, which derive in cumbersome structures. For high integrability MMIC devices, different 2-D approaches should be used such as microstrip or coplanar feeds.

In this letter, Section 2 presents an ENZ tunnel with microstrip coupling for high integrability applications. Section 3 explains the theoretical formulation of the ENZ tunnel circuit. Section 4 provides the complete design procedure, simulation results of the ENZ tunneling circuit, and a methodology to extract the effective permittivity and propagation constants in the tunnel is described. Moreover, the dependence on external quality factor and tunnel to feed height ratio of the tunnel circuit is presented. Section 5 presents the simulated and measured results of the tunnel structure. This tunneling structure plays crucial role in developing high integrability microwave devices. This tunneling device can be used in the design of the microwave filters, Notch filters, Oscillators, Diplexers etc. Apart from these devices, this can be used for waveguide bends [1, 6], antenna matching circuits [7] and dielectric sensing applications [8].

Especially these ENZ tunnels can be utilized in microwave filter applications. This technology has a potential advantage in miniaturization as energy can be tunneled through a narrow waveguide at a particular frequency which is independent of its total length. Moreover, compared to other metamaterial structures, based on microstrip or coplanar configurations, radiation losses are reduced.

2. ENZ TUNNELING CIRCUIT USING MICROSTRIP COUPLING

ENZ tunneling behavior can be accomplished by using a double negative metamaterial or waveguide technology. A double negative metamaterial is operated at the transition frequency between the right hand and left hand propagation. In waveguide technology, the effective permittivity of a TE_{10} rectangular waveguide filled with a dielectric of relative permittivity (ε_r) is given below [9]

$$\varepsilon_{eff} = n^2 - \frac{c^2}{4\varepsilon_r f^2 w_t^2} \tag{1}$$

where n is the refractive index of the filling material, ε_r is the relative permittivity of the material, c is the speed of light in vacuum, W_t is

the waveguide H-plane width, and f is the operation frequency. The effective permeability (μ_{eff}) remains constant with a value of μ_o.

From the above equation, it is observed that below cutoff frequency the effective permittivity is negative ($\varepsilon_{eff} < 1$), above cutoff frequency, it is positive ($\varepsilon_{eff} > 0$); thus at cutoff frequency, $\varepsilon_{eff} \sim 0$. And also at cutoff frequency, the propagation constant is zero ($\beta = 0$) which leads to an infinite phase velocity [5]. This gives rise to perfectly matched propagation. Alu et al. [8], extended this concept to resonant-like ENZ waveguide tunnels in which the tunneling ("resonant") frequency is completely independent of the length of the tunnel; hence, its size can be miniaturized. They named this tunneling as supercoupling phenomenon. Alu et al. [10], explained this super coupling based on the line impedance matching of an ultra narrow tunnel having ENZ material using waveguide technology.

Super coupling phenomenon has some distinct features different from conventional resonance: It is fundamentally independent of the length of the tunnel and its overall geometry, provided that the total longitudinal cross sectional area of the ENZ channel remains sufficiently small. Since the electromagnetic wave does not really propagate in an ENZ medium, but rather tunnels through it with an effectively infinite phase velocity, the transmission properties of the channel are simply determined by its input and output faces. Figure 1(a) shows the geometry of the ENZ tunneling circuit using waveguide method. It consists of two parallel plate waveguides of height h_{wg} filled with effective permittivity (ε_{wg}) connected by a narrow tunnel of h_t ($\ll h_{wg}$) and effective permittivity (ε_t). Figure 1(b) depicts the E-field distribution along the propagation direction at the tunneling frequency.

The tunnel structure described above is adopted using microstrip technology. This structure consists of a microstrip-tunnel-microstrip transition as shown in Figures 2(a) and (b). The metallic waveguide of height (h_t) connected to the microstrip lines act as the ENZ tunnel. In order to have tunneling, a very abrupt discontinuity between the microstrip feed line and the tunnel must exist to ensure that only signals around the ENZ frequency are tunneled through while others are reflected back. Hence, the microstrip substrate height should be much larger than the tunnel height ($h_\mu \gg h_t$). In addition to that a metallic strip of height (h_m) is used as shown in Figure 2(c) at tunnel and microstrip interface, to confine more electromagnetic energy in the tunnel and to avoid leakage. A small gap is maintained between the heights of metallic strip (h_m) and tunnel (h_t) to have proper ground.

The fundamental mode of wave propagation in a microstrip is quasi TEM mode. Typically, in operation of the circuit a quasi TEM

mode wave propagating in the microstrip converts into a TE_{10} mode inside the tunnel at the tunneling frequency. Therefore a TE_{10} mode of wave propagation exists inside the tunnel at tunneling frequency.

3. THEORETICAL FORMULATION

A characteristic impedance model for the configuration shown in Figure 1 has been explained in detail [11] which is also applicable to the current design. Figure 3 shows the equivalent circuit of the tunnel structure using transmission line approach.

This transmission line model is derived such that the tunnel region can be replaced by a region having an impedance $(Z_t = (h_\mu/h_t)Z_\mu)$ where h_μ/h_t is the ratio of the microstrip and tunnel heights. In addition, there is a shunt admittance $Y = jB$ at the interface between the microstrip and the tunnel. The reflectance of the ENZ tunnel
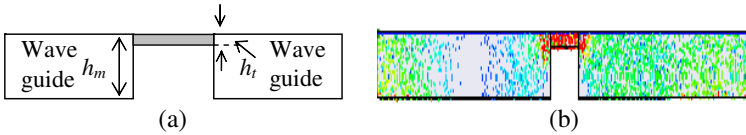

Figure 1. (a) Schematic of the ENZ approach using waveguide technology, (b) E-field pattern of the tunnel structure.
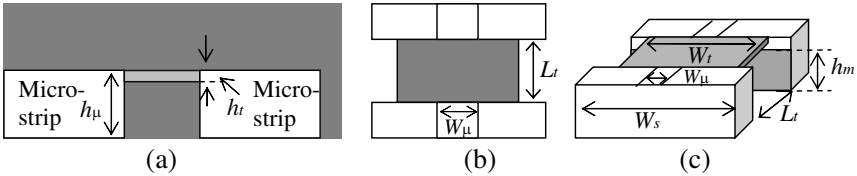

Figure 2. (a) Schematic of the ENZ tunneling circuit using microstrip technology (side view), (b) top view, (c) metallic strip at the tunnel and microstrip interface.
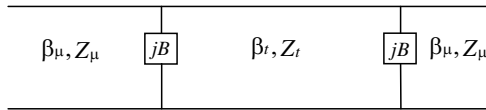

Figure 3. Schematic of the ENZ tunneling circuit based on transmission line method.

circuit based on the simplified model described in is given below.

$$R = \frac{\Gamma \left(1 - e^{i2\beta_t d}\right)}{1 - \Gamma^2 e^{i2\beta_t d}} \tag{2}$$

where $\Gamma = \left(\frac{Z_t//(-iB) - Z_\mu}{(Z_t//(-iB) + Z_\mu)}\right)$ and $Z_t//(-iB) = \left(\frac{-iBZ_\mu}{-iB + Z_\mu}\right)$. Γ is the reflection coefficient between the microstrip substrate height and the channel. β_t is the wave vector inside the tunnel. Z_μ and Z_t are the effective wave impedances outside and inside the narrow channel respectively. When ε tends to zero, the characteristic impedance of the zero index material may take on a finite value, which could be different from the impedance of the adjacent regions. However, since β_t tends to zero, the reflection coefficient vanishes, indicating the tunneling of the wave across the channel. Thus, the tunneling is based on the anomalous line impedance match provided by the ENZ material.

4. TUNNEL DESIGN AND EFFECTIVE PARAMETER EXTRACTION

The width of the ENZ tunnel operating at TE_{10} mode is given by

$$W_t = \frac{c}{2f_0\sqrt{\varepsilon_r}} \tag{3}$$

where f_o is the tunneling frequency, c is the speed of light and ε_r is the relative permittivity.

The length of the tunnel is independent of frequency due to its quasi-static behavior. Nevertheless, when the length of the tunnel is half wavelength, a conventional resonance can be excited, therefore it is important to chose the tunnel length small enough such that this resonance is out of our band of interest.

A tunnel centered at 2.6 GHz was designed and fed by different microstrip lines with different substrate heights. The substrate chosen for both the tunnel and microstrip is RT Duroid 5880 with permittivity of 2.2, loss tangent of 0.001. The characteristic impedance of the input/output microstrip is $50\,\Omega$. The dimensions of the tunnel structure shown in Figure 2(a) are $W_s = 42\,\text{mm}$, $W_t = 40\,\text{mm}$, $W_\mu = 10\,\text{mm}$, $h_\mu = 3.2\,\text{mm}$, and h_t is changed from 0.4 mm to 1.6 mm.

It is very important to note that Q-factor plays an important role for the MMIC devices. In order to analyze the Q-factor of the tunneling circuit, firstly a proper analysis on the height of the tunnel to the microstrip substrate ratio should be done. Simulations were performed on various height ratios of microstrip and tunnel thickness using an electromagnetic wave simulator based on Finite Element Method [12]. Figure 4(a) shows the simulated transmission parameters of the tunnel

structure for various height ratios. As the tunnel height increases, the tunneling peak becomes broader. The variation of quality factor of the tunnel with ratio of the height of the tunnel and the microstrip substrate is presented in Figure 4(b). It is clear that as the height of the tunnel increases the Q-factor decreases. When the height ratio approaches 1, the line behaves as a transmission line. For high external Q, extremely thin tunnels should be chosen.
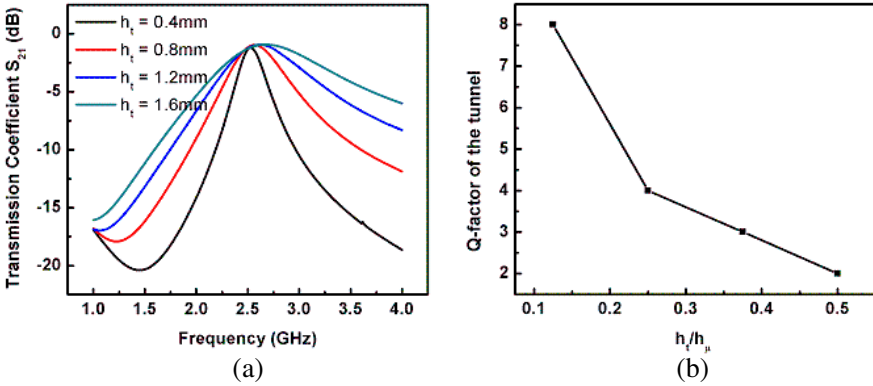

Figure 4. (a) Transmission coefficient of the ENZ tunnel structure for various height ratios. (b) Variation of quality factor of the tunnel with ratio of the height of the tunnel and the microstrip substrate.
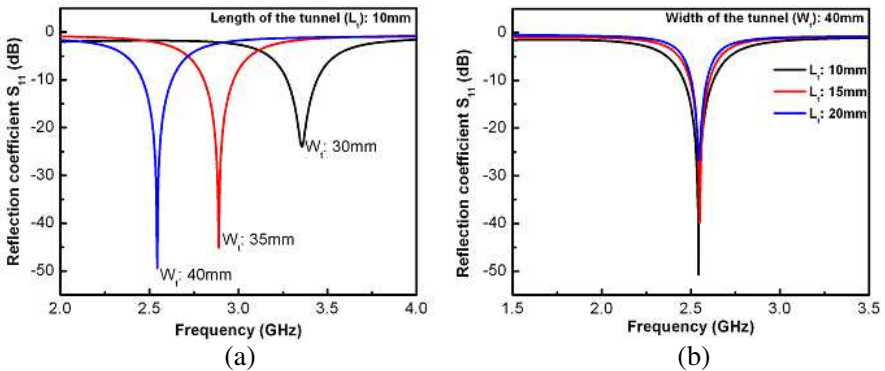

Figure 5. (a) Simulated reflection coefficient of the ENZ tunnel structure for various widths. (b) Simulated reflection coefficient of the ENZ tunnel structure for various lengths.

An optimized height ratio is chosen such that it has excellent transmission at the tunnel frequency and for ease of fabrication. In
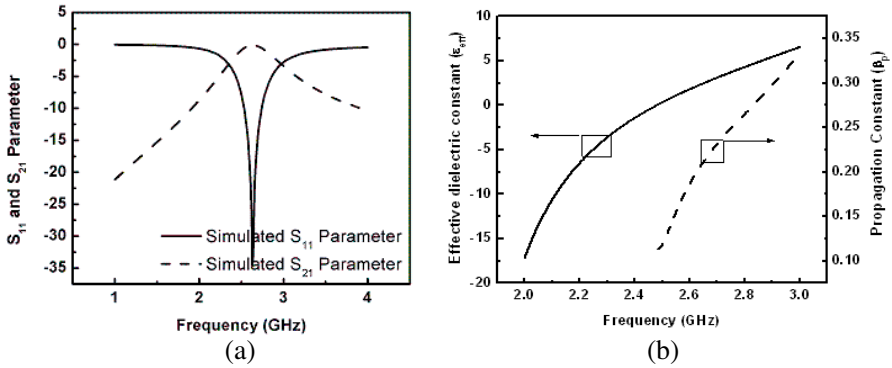
Figure 6. (a) Simulated and measured reflection and transmission coefficients of the optimized ENZ tunnel. (b) Extracted dielectric permittivity and propagation constant parameters from the simulated S-parameters of the ENZ tunnel.

our case the tunnel height is chosen to be $h_t = 0.7\,\text{mm}$ ($h_t/h_\mu = 0.22$). The dimensions of the optimized tunnel structure are $W_s = 42\,\text{mm}$, $W_t = 40\,\text{mm}$, $W_\mu = 10\,\text{mm}$, $L_t = 10\,\text{mm}$ $h_\mu = 3.2\,\text{mm}$, $h_t = 0.7\,\text{mm}$, $h_m = 2.48\,\text{mm}$. Figure 6(a) shows the simulated reflection and transmission coefficients of the optimized tunnel structure. In order to prove that tunneling mainly depends on the width of the tunnel. Simulations are performed by varying the tunnel widths from 20 mm to 40 mm keeping the length of the tunnel as 10 mm. And also simulations are performed for various tunnel lengths (10 mm to 20 mm) by keeping width of the tunnel as 40 mm. Figures 5(a) and 5(b) show the simulated reflection coefficients of the tunnel structure for various tunnel widths and lengths respectively.

From the above figures, it is observed that, as the tunnel width increases, the resonant frequency decreases. It is evident that the resonance is mainly due to the tunnel width but not from the microstrip feed. It is also clear that resonant frequency of the tunnel structure is independent of length of the tunnel which is very important for the miniaturization applications.

The effective permittivity ($\varepsilon_{\textit{eff}}$) of the tunnel structure shown in Figure 1 was extracted from S_{11} and S_{21} simulated parameters using Equations (4), (5) and (6) [13]. The reflection/transmission and scattering parameters are related as given below

$$S_{11} = \frac{\Gamma\left(1 - T^2\right)}{1 - \Gamma^2 T^2}; \quad S_{21} = \frac{T\left(1 - \Gamma^2\right)}{1 - \Gamma^2 T^2} \tag{4}$$

The above equation can be rearranged and written in the following

form

$$\Gamma = K \pm \sqrt{K^2 - 1}; \quad T = \left(\frac{S_{11} + S_{21} - \Gamma}{1 - (S_{11} + S_{21})\,\Gamma} \right) \qquad (5)$$

where $\Gamma = \left(\frac{Z_{eff} - Z_0}{Z_{eff} + Z_0} \right)$ is the reflection coefficient and $T = e^{(-\gamma d)}$ is the transmission coefficient. $\gamma = [\ln(1/T)]/d$; $K = \frac{S_{11}^2 - S_{21}^2 + 1}{2 S_{11}}$; γ_0 is the free space propagation constant; λ_0 is the free space wavelength. Z_{eff} is the effective impedance of the tunnel structure and Z_0 is the free space impedance. From the above equation the effective dielectric permittivity can be derived as

$$\varepsilon_{eff} = \frac{\gamma\,(1 - \Gamma)}{\gamma_0 (1 + \Gamma)} \qquad (6)$$

Furthermore, by using Equation (7) the phase constant is extracted.

$$\beta = \arccos \left(\frac{1 - S_{11} S_{22} + S_{21}^2}{2 S_{21}} \right) \qquad (7)$$

The effective dielectric constant and the propagation constant parameters of the ENZ structure are extracted from the simulated S-parameters of the optimized structure. The variation of these parameters with frequency is shown in Figure 6(b). It is clear that the effective dielectric constant has zero values near the tunneling frequency (2.6 GHz) and also the propagation constant has near zero (0.11) which satisfies the properties of ENZ behavior.

5. RESULTS AND DISCUSSION

The proposed structure with optimized height ratio is fabricated using conventional PCB milling machine. The substrate is Duriod-5880 substrate with dielectric constant $\varepsilon_r = 2.2$, loss tangent $\delta = 0.001$, thickness $h = 3.2$ mm. The plasmonic tunnel was machined as per dimensions and all the layers were properly metalized. Figure 7(a) shows a photograph of the ENZ structure using microstrip technology.

Measurements are carried out using Agilent PNA Series microwave Vector Network Analyzer (E8361A). Figure 7(b) shows the simulated and measured reflection and transmission coefficients of the proposed structure. Results demonstrate that the fabricated structure has a shift in the desired frequency about 55 MHz. It can be seen that the structure at tunneling frequency has low insertion loss 1.01 dB (measured) and 0.125 dB (simulated) the attenuation characteristic show more than 35 dB (simulated) and 15 dB (measured). The measured results almost comply the simulated results and only a small frequency offset and a different insertion and reflection losses are due to the fabrication tolerance.
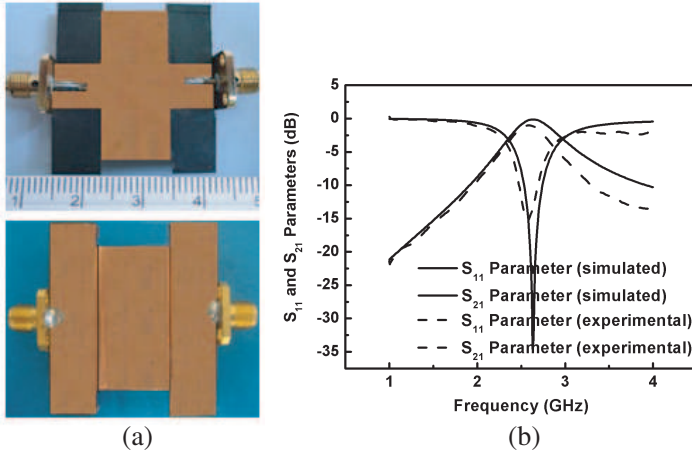
Figure 7. (a) Photograph of the ENZ tunneling circuit (top view and bottom view). (b) Simulated and measured reflection and transmission coefficients of the optimized ENZ tunnel.

6. CONCLUSIONS

A novel ENZ tunneling circuit using microstrip technology is presented in this letter. Simulations were performed for various height ratios. An optimized ratio is chosen which has very good transmission and Q-factor at the tunnel frequency. The measurement results have shown good agreement with the theoretical results. We believe this newly proposed novel compact ENZ tunneling circuit can be used in a wide range of microwave and millimeter wave applications.

REFERENCES

1. Silveirinha, M. G. and N. Engheta, "Tunneling of electromagnetic energy through sub-wavelength channels and bends using epsilon-near-zero (ENZ) materials," *Phys. Rev. Lett.*, Vol. 97, No. 15, 157403-1–157403-4, Oct. 2006.

2. Alù, A. and N. Engheta, "Achieving transparency with plasmonic and metamaterial coatings," *Phys. Rev. E*, Vol. 72, No. 1, 016623-1–016623-9, Jul. 2005.

3. Alù, A., M. G. Silverinha, A. Salandrino, and N. Engheta, "Epsilon-near-zero metamaterials and electromagnetic sources: Tailoring the radiation phase pattern," *Phys. Rev. B*, Vol. 75, No. 15, 155410-1–155410-13, Apr. 2007.

4. Silveirinha, M. G. and N. Engheta, "Theory of supercoupling, squeezing wave energy, and field confinement in narrow channels and tight bends using ε-near zero materials," *Phys. Rev. B*, Vol. 76, No. 24, 245109-1–245109-17, Dec. 2007.

5. Edwards, B., A. Alù, M. E. Young, M. G. Silveirinha, and N. Engheta, "Experimental verification of epsilon-near-zero metamaterial coupling and energy squeezing using a microwave waveguide," *Phys. Rev. Lett.*, Vol. 100, No. 3, 033903-1–033903-4, Jan. 2008.

6. Edwards, B., A. Alù, M. G. Silveirinha, and N. Engheta, "Reflectionless sharp bends and corners in waveguides using epsilon-near-zero effects," *J. Appl. Phys.*, Vol. 105, No. 4, 044905-1–044905-4, Feb. 2009.

7. Alù, A. and N. Engheta, "Antenna matching in ε-near-zero metamaterial channels," *IEEE International Workshop on Antenna Technology, iWAT 2009*, 1–4, Mar. 2–4, 2009.

8. Alù, A. and N. Engheta, "Dielectric sensing in ε-near zero narrow waveguide channels," *Phys. Rev. B*, Vol. 78, No. 4, 045102-1–045102-5, Jul. 2008.

9. Rotman, W., "Plasma simulation by artificial dielectrics and parallel-plate media," *IRE Trans. Antennas Propag.*, Vol. 10, No. 1, 82–95, Jan. 1962.

10. Alù, A., M. G. Silveirinha, and N. Engheta, "Transmission-line analysis of ε-near-zero–filled narrow channels," *Phys. Rev. E*, Vol. 78, No. 4, 016604-1–045102-10, Jul. 2008.

11. Collin, R. E., *Field Theory of Guided Waves*, 2nd edition, IEEE Press, New York, 1980.

12. Ansoft HFSS Software, version.11.

13. Lubkowski, G., R. Schuhmann, and T. Weiland, "Extraction of effective metamaterial parameters by parameter fitting of dispersive models," *Microwave Opt. and Technol. Lett.*, Vol. 49, No. 2, 285–288, Feb. 2007.